Analysis of deformation mechanism with stress-strain behavior of geogrids by FEM

Jeon, H. Y.
Division of Nano-Systems Engineering, INHA University, Incheon, Korea

Ko, E. H., Yoo, S. E & Kim, S. Y.
Department of Textile Engineering, INHA University Graduate School, Incheon, Korea

Lee, K. Y.
Department of Civil Engineering, University of Dongseo, Busan, Korea

Keywords: finite element analysis, junction strength, stress distribution, wide-width tensile behaviors, Visual FEA/Edu program, contour image

ABSTRACT: In this study, junction strength, stress distribution of geogrids and the test improvement of wide-width tensile strength were interpreted by FEA program. Used by Visual FEA/Edu program, it effected an inspection of evidence that compared actual test data with FEA program data. Stress distribution effect appeared in transverse ribs, Warp knitted type was better than Woven type in stress distribution effect, contour image in FEA program indicated change of stress in adjacent point and the transformation was predicted by FEA simulation. In wide-width tensile strength test, though stress and data in transformation were related to the actual data was confirmed, but it is good that data in actual test utilized in FEA because the result data was different from mesh data made by FEA program.

1 INTRODUCTION

Geogrids are widely used as efficient reinforcing materials in soil retaining wall, embankment and ground reinforcement because of their excellent pullout resistance, shear stress between soil structures. (Ling et al. 2005) Before examination geogrids reinforcement effects to soil structure, it is necessary to analyze the stress distribution effect of geogrids. (Giroud 2002, Koerner and Soong 2001) To apply this to finite element analysis, it is seen that deformation mechanism could be predicted for interpretation of junction and tensile behaviors. In this study, it is analyzed stress distribution effects and junction behaviors by finite element program, Visual FEA/Edu. and approved the validity of this analysis through comparison between experimental data and the prediction values of this program.

2 MODELLING OF FINITE ELEMENT ANALYSIS

Warp knitted and woven type geogrids of design strength, 6ton/m which generally used for soil retaining wall system in Korea were selected. Schematics of geogrid pattern for finite element analysis and aperture size of geogrids is shown in Fig. 1 and Table 1, respectively.

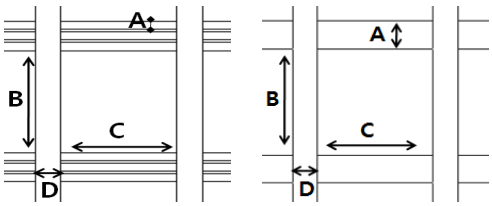

(a) Warp knitted type (b) Woven type

Figure 1. Schematics of geogrids specimen.

Table 1. Aperture size of geogrids (mm)

Geogrid	Warp knitted type				Woven type			
Component	A	B	C	D	A	B	C	D
Value	1.5	19	18	4	5	19	19	4

Four geogrid ribs were selected for finite element network composition to be considered specimen size of wide-width tensile test. Shape of geogrid specimen for finite element analysis is square type to be considered the uniform stress distribution. The finite element network compositions for junction and tensile strength prediction by using square type are shown in Fig. 2 and 3, respectively.

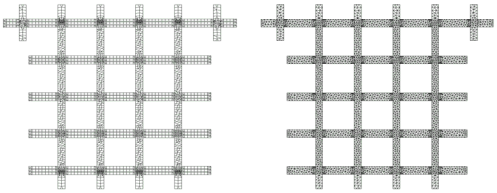

(a) Warp knitted type (b) Woven type

Figure 2. Schematics of finite element network structure for junction strength analysis of geogrids.

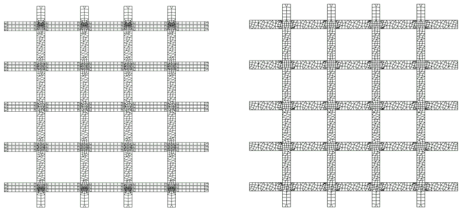

(a) Warp knitted type (b) Woven type

Figure 3. Schematics of finite element network structure for tensile strength analysis of geogrids.

3 COMPOSITION OF FINITE ELEMENT ANALYSIS

Finite element network model for junction strength analysis of geogrids are shown in Fig. 4. Junction strength of geogrids to be evaluated in accordance with GRI GG2 and are represented in Table 2. 10%, 20% and 40% of this junction strength were applied to finite element network model. During junction strength test, real stress applied part of geogrid is shown as the specimen clamped area e.g., both square parts of Fig. 4 which the specimen is fixed. Also, stress transition part of geogrid is shown in the circular area of Fig. 4.

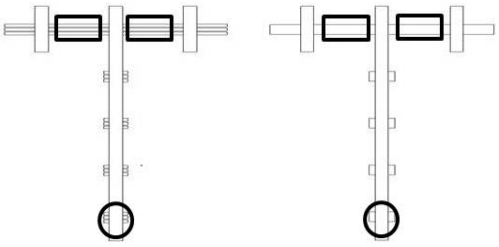

(a) Warp knitted type (b) Woven type

Figure 4. Stress applied part of geogrids for finite element analysis

Table 2. Junction strength of geogrids

Geogrid	Warp knitted type	Woven type
Junction Strength(kg)	169	180

For analysis of wide-width tensile strength as same as junction strength, 40%, 50% and 60% of evaluated wide-width tensile strength by ASTM D4565 in Table 3 were applied to finite element network model. Finite element network model for wide-width tensile strength analysis of geogrids are shown in Fig. 5.

Table 3. Wide-width tensile strength of geogrids

Geogrid	Warp knitted type	Woven type
Wide-width tensile Strength(kg)	1656.8	1655.5

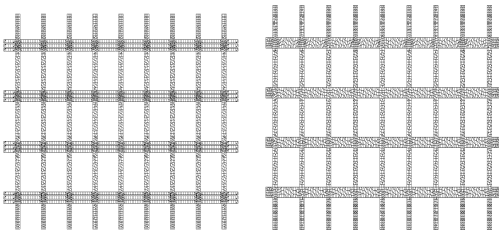

(a) Warp knitted type (b) Woven type

Figure 5. Schematics of finite element network structure for wide-width tensile strength analysis of geogrids..

4 RESULTS AND DISCUSSION

4.1 *Prediction of junction and wide-width tensile behaviors*

Predicted deformation shapes of warp knitted and woven type geogrids in case of 20% of junction strength of Table 1, 34kg and 36kg being applied were shown in Fig. 6 and 7, respectively.

The reason why this strength was applied is that the evaluated junction strength by GRI GG2 would be almost similar to the result by finite element analysis. In here, effect of stress distribution would be predicted larger due to the different junction part formation though predicted deformation does not show significant difference between two geogrids. Stress changes at X- and Y-axis by finite element analysis for interpretation of stress distribution effect of geogrids were shown as contour image in Fig. 8~11. Through contour image interpretation, it is seen that stress distribution effects were larger on junction bonding areas than other parts of geogrids. Also, stress distribution effects for both geogrids were larger at Y-axis than X-axis and the difference between X and Y-axis was larger in warp knitted

type geogrid than woven type geogrids. As explained before, this difference is mainly due to the different junction part formation of geogrids.

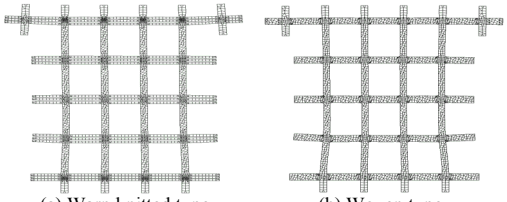

(a) Warp knitted type (b) Woven type

Figure 6. Schematics of predicted deformation of finite element network structure for junction strength analysis of geogrids.

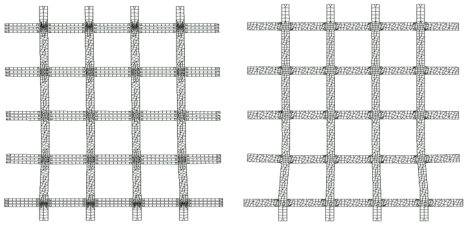

(a) Warp knitted type (b) Woven type

Figure 7. Schematics of predicted deformation of finite element network structure for wide-width tensile strength analysis of geogrids.

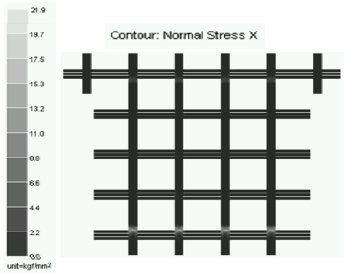

(a) X-axis

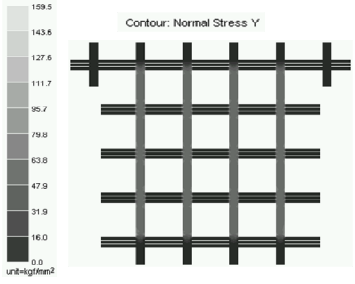

(b) Y-axis

Figure 8. Schematics of stress distribution of finite element network structure for junction strength analysis of warp knitted type geogrid.

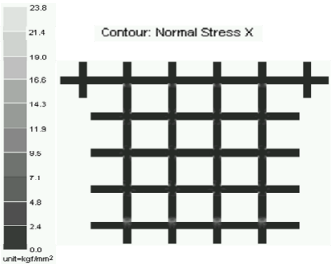

(a) X-axis

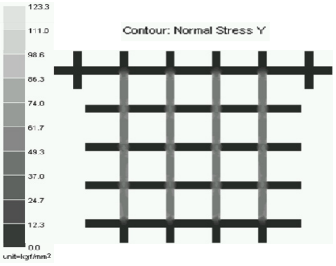

(b) Y-axis

Figure 9. Schematics of stress distribution of finite element network structure for junction strength analysis of woven type geogrid.

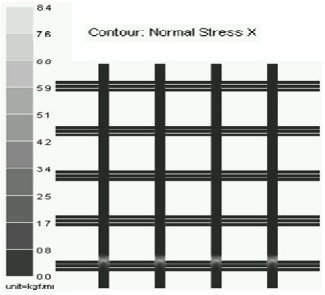

(a) X-axis

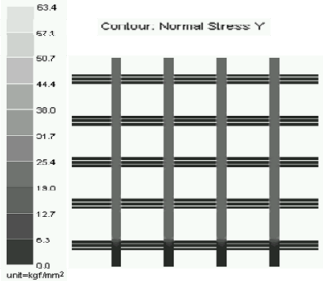

(b) Y-axis

Figure 10. Schematics of stress distribution of finite element network structure for wide-width tensile strength analysis of warp knitted type geogrid.

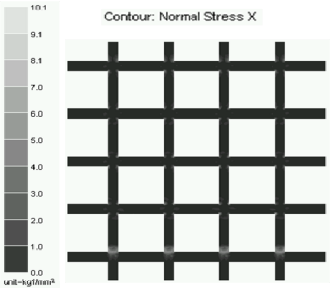

(a) X-axis

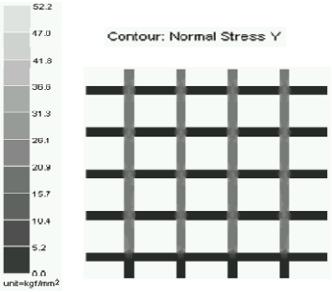

(b) Y-axis

Figure 11. Schematics of stress distribution of finite element network structure for wide-width tensile strength analysis of woven type geogrid.

Fig. 12 shows the predicted deformation of warp knitted type geogrid in case of 20% of evaluated junction strength of Table 2 under condition that specimen clamped in square areas of Figure 4. This can be explained that although predicted deformation by finite element analysis should be occurred as shown in Fig. 12 because stress in these square areas transfers along the horizontal direction under clamping However, this interpretation is very different from real test phenomena and therefore, stress applied part must be changed to junction bonding part as shown in Fig. 13. This changed junction bonding part is just equivalent to stress transferring place. In Fig. 13, the arrow directed parts mean the real stress added place and Fig. 14 means the predicted deformation by changed stress transferring of finite element analysis of geogrid. in clamping part As one of the analysis, contour image analysis is a useful methods to interpret stress transfer on junction bonding parts of geogrid. Fig. 15 shows the stress contour image of geogrids at X-axis by finite element analysis and junction strength is the best on the stress transferring axis. Furthermore, junction strength at the cross point of X- and Y-axis shows the best though stress is transferred along the stress action axis. It is seen that this is due to stress dispersion around the junction part along two axes and this phenomenon is the specific property of warp knitted junction bonding. On the other hand, it is predicted that stress dispersion of woven type geogrid at junction point would be smaller than warp knitted geogrid because junction part of woven type geogrid is made of not cross linking but weaving of warp and weft yarns. This is the cause of strong junction bonding by protection of junction point sliding with PVC coating.

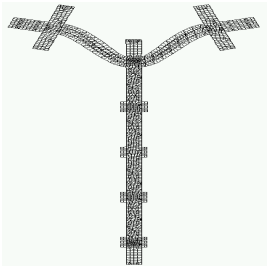

Figure 12. Schematics of predicted deformation of finite element analysis of geogrid in clamping part.

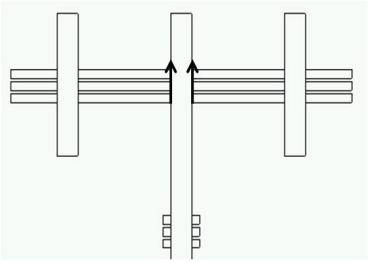

Figure 13. Schematics of changed stress transferring of finite element analysis of geogrid in clamping part.

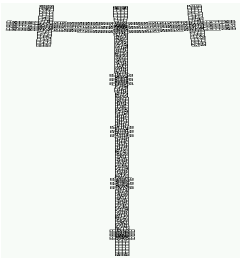

Figure 14. Schematics of predicted deformation by changed stress transferring of finite element analysis of geogrid in clamping part.

Contour images on 40% and 60% wide-width tensile strength of Table 3 for warp knitted and woven type geogrids are shown in Fig. 16, respectively. And Fig. 17 shows the predicted deformation of finite element network structure of geogrids with wide-width tensile strength. From this, it can be assumed that breakage and failure of geogrids may be occurred at the point having the maximum contour image value

by considering the properties of finite element analysis.

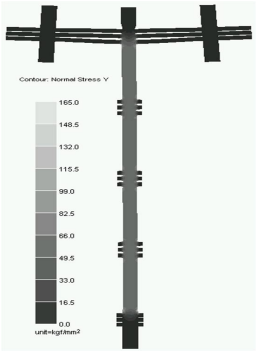

Figure 15. Stress contour image of warp knitted type geogrid in Y-axis

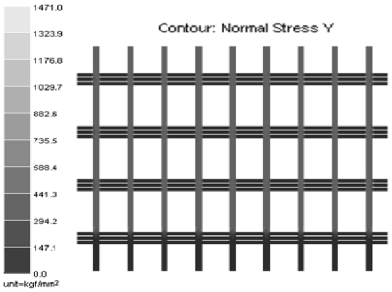

(a) Warp knitted type

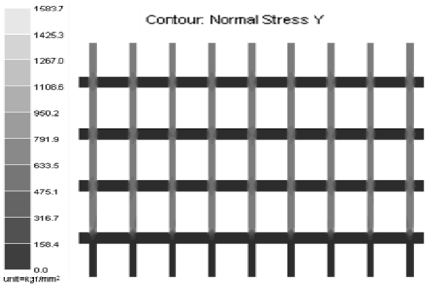

(b) Woven type

Figure 16. Stress contour image of geogrids in Y-axis with wide-width tensile strength.

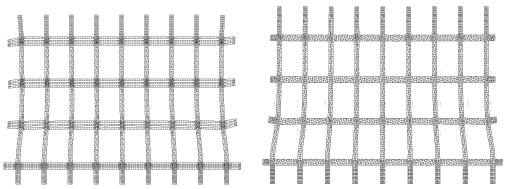

(a) Warp knitted type (b) Woven type

Figure 17. Schematics of predicted deformation of finite element network structure of geogrids with wide-width tensile strength.

5 CONCLUSION

It is confirmed that junction strength of warp knitted and woven type geogrids by finite element analysis is very similar to experimental data by index junction strength test, GRI GG2. And stress distribution for 20% application of evaluated junction strength to finite element analysis would be almost as same as experimental data. Through contour image analysis, it is possible to predict the stress change and deformation at junction point of geogrids. Also, larger stress dispersion occurred at Y-axis than X-axis for junction and wide-width tensile strength analysis by contour image and this is due to real stress transfer to Y-axis. Stress dispersion effects mainly occurred at each rib cross point and warp knitted type geogrid showed better stress dispersion effect. Finally, it is reasonable to apply real experimental values to finite element analysis because the prediction value may be different how to design the finite element network and distribute the finite elements with the shape of geogrid.

ACKNOWLEDGEMENT: This work was supported by grant No. RTI04-01-04 from the Regional Technology Innovation Program of the Ministry of Knowledge Economy (MKE).

REFERENCES

Ling, H. I. et al. 2005. Geosynthetics and geosynthetics-engineered soil structures", *McMat 2005 Conference*, Baton Rouge, Lousiana, US, pp. 9-124.

Giroud, J. P. 2002. Lessons Learned from successes and failures Associated with Geosynthetics. *Proc. of 2nd European Geosynthetics Conference*, Vol. 1, pp. 77-118.

Koerner, R. M. and Soong, T. Y. 2001. Geosynthetic reinforced segmental retaining walls. *Geotextiles and Geomembranes*, Vol. 19, No. 6, pp. 359-386.